MR Imaging of Fe-Co Nanoparticles, Magnetotactic Bacteria and Fe_3O_4 Microparticles for Future Drug Delivery Applications

Ouajdi Felfoul Student Member, IEEE, Pierre Pouponneau, Jean-Baptiste Mathieu Student Member, IEEE, and Sylvain Martel*, Senior Member, IEEE

NanoRobotics Laboratory, Department of Computer Engineering and Institute of Biomedical Engineering, École Polytechnique de Montréal (EPM), Campus of the Université de Montréal, Montréal, Canada

***Abstract* — Magnetic resonance imaging characteristics of novel potential drug delivery agents are investigated. Candidate carriers considered in this study are iron-cobalt (Fe-Co) nanoparticles, magnetotactic bacteria (MTB), and magnetite (Fe_3O_4) microparticles. The micro and nanoparticles are highly magnetic and can be steered using gradient coils. MTB, on the other hand, are microorganisms that naturally follow the magnetic field lines through a mechanism called magnetotaxis. These carriers share the capability to be controlled by magnetic field and to be detected on MR images.**

Keywords — ***MR imaging, Fe-Co nanoparticles, magnetotactic bacteria, Fe_3O_4 microparticles, drug delivery.***

I. Introduction

Many strategies have been proposed to target anticancer agents to tumors using magnetic carrier particles. Generally, nano or micro magnetic particles are injected upstream with the blood flow and captured using an applied local magnetic field [1]. Magnetic Resonance Imaging (MRI) has the advantage to be sensitive to magnetic particles and thus could be used as a guiding as well as a monitoring tool. In fact, the possibility to use MRI gradients as a means of propulsion for microdevices in blood vessels has already been proven by automatic navigation of a ferromagnetic particle along a predetermined path *in vivo* [2],[3]. Magnetic particles affect the longitudinal relaxation time (T_1) and transversal relaxation time (T_2) of the protons in their vicinity helping to achieve a pronounced contrast with regard to tissue lacking these compounds. The magnetic properties of the carrier as well as its dimension are the most important factors affecting the MR-images properties. In this study we investigate T_1 and T_2 weighted MR-images of Fe-Co nanoparticles, Fe_3O_4 microparticles and magnetotactic bacteria (MTB).

Microparticles could mimic a biodegradable micro carrier loaded with nanoparticles. MTB contain an intracellular magnetite chain (Fe_3O_4) [4], they are self-propelled and could potentially reach deep tumor area as it is the case with other type of bacteria [5]. For complementary purpose, these carriers can be integrated in a single device. As a matter of fact, different imaging parameters must be considered regarding the nature of the magnetic particles to be used.

This project is supported in part by a Canada Research Chair (CRC) in Micro/Nanosystem Development, Fabrication and Validation, the Canada Foundation for Innovation (CFI) and the National Sciences and Engineering Research Council of Canada (NSERC).

Contact author: **sylvain.martel@polymtl.ca.*

II. Materials and Methods

A. *Fe-Co Nanoparticles Preparation*

Different concentrations have been prepared for each material. Fe-Co nanoparticles coated with oleic acid were provided by Inorganic Chemistry III Laboratory of Bielefeld University (Germany) [6]. The metal content was 25 mg/ml and the ratio was Fe/Co = 1:1. Mean nanoparticles diameter was 2.9 nm. The nanoparticles were stabilized in a hexane solution used as medium for imaging experiments. Five samples of 1 ml were prepared with concentrations, 9.375 mg/ml, 12.5 mg/ml, 18.75 mg/ml, 21.875 mg/ml, and 25 mg/ml.

B. *MTB Preparation*

MTB has been grown for 10 days in 1.5 liters of liquid medium [7]. The bacteria were concentrated by centrifugation into a final volume of 100 ml. Five different samples where prepared by adding 10%, 30%, 50% and a 70% of the medium to the concentrated solution. Qualitative observation of bacterial motility and response to the magnetic field before and after concentrating was performed using a Zeiss Imager.Z1 microscope in order to validate the vitality and magnetotaxis after centrifugation.

C. *Fe_3O_4 Microparticles Preparation*

The Fe_3O_4 microparticles suspension (Bangs Laboratories [8]) is made of superparamagnetic Fe_3O_4 mixed with polymer particles (10.8µm average size) suspended in distilled water. Weigh fraction of Fe_3O_4 (m_{sat} = 92emu/g) inside the particles is above 90%, corresponding to a minimum particle magnetic moment of 82.8 emu/g. Five samples of 1 ml were prepared with concentrations 0.19 mg/ml, 0.25 mg/ml, 0.33 mg/ml, 0.44 mg/ml, 0.59 mg/ml. The control sample, without magnetic particles, was prepared by centrifugation of a magnetite suspension vial and retrieving 1 ml of suspending DI water. A 1 ml of every sample of the three materials was inserted into a 2 ml Progene microtube prior to MR-imaging.

D. *Fe_3O_4 Microparticles Preparation*

Images were run under a Siemens Avanto 1.5 T scanner using the wrist antenna. T_1 weighted spin echo sequence

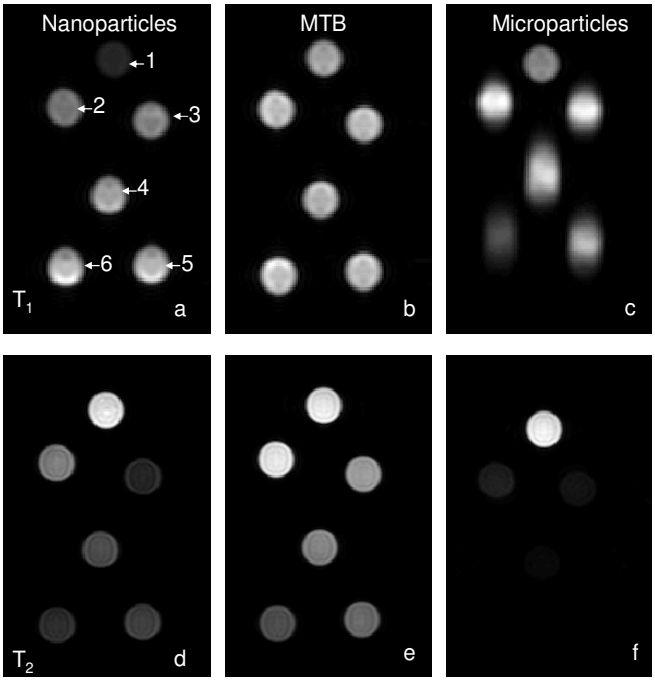

Fig. 1. T_1 and T_2 images of samples of Fe-Co nanoparticles, magnetotactic bacteria (MTB), and Fe_3O_4 microparticles. Sample 1 to 6 (as numbered in a) show increasing concentrations starting from medium without magnetic particles (sample 1). T_1 weighted spin echo sequence with TE/TR = 11/450 ms and T_2 weighted fast spin echo sequence with TE/TR = 135/5096 ms were used.

parameters were: TE = 11 ms and three different TR = 450/550/700ms, a slice thickness of 20mm, and a pixel spacing of 0.586mm. T2 weighted fast spin echo sequence parameters were: TE = 96/125/135 ms, TR = 5096 ms and a pixel spacing of 0.293 mm.

III. RESULTS

A. *T1-contrast*

Fe-Co nanoparticles show a signal enhancement in T_1 weighted images as the concentration of the magnetic particles is increased as depicted in Figure 1a. Fe_3O_4 microparticles, however, cause a blurring on T_1 weighted images as depicted in Figure 1c. This image artifact is in part caused by the fact that we vortexed the samples since the microparticles tend to aggregate in the solution. Samples containing MTB show signal enhancement compared to the medium in T_1-weighted images as depicted in Figure 1b. However, this signal enhancement didn't change significantly with higher cell concentrations.

B. *T_2-contrast*

The effect of the magnetic particles that we imaged is more evident on T_2-weighted images than T_1-weighted images. As

Table 1. T_2-relaxation values for different concentrations of Fe-Co nanoparticles and MTB calculated from signal ratio measurements.

	Concentrations		T_2 (ms)	
	Fe-Co nanoparticles (mg/ml)	MTB (cells/ml) $\times 10^7$	Fe-Co nanoparticles	MTB
Medium (sample1)	0	0	1461	646
sample2	9.375	2.2	122	305
Sample3	12.50	3.5	75	203
Sample4	18.75	4.8	92	172
sample5	21.875	6.2	88	156
Sample6	25	6.7	71	114

depicted in Figure 1d, Fe-Co nanoparticles cause a signal loss for higher concentration. The same phenomena is observed for the MTB samples, as the concentration of bacteria increases, the signal decay becomes important and a severe signal loss in T_2 weighted images is observed as given by Figure 1e. A complete signal loss is observed in T_2-images of Fe_3O_4 microparticles as depicted in Figure 1f. For an enhanced illustration, the signal intensity decreases for the T_2-contrast of the Fe-Co nanoparticles as well as the MTB is plotted in Figure

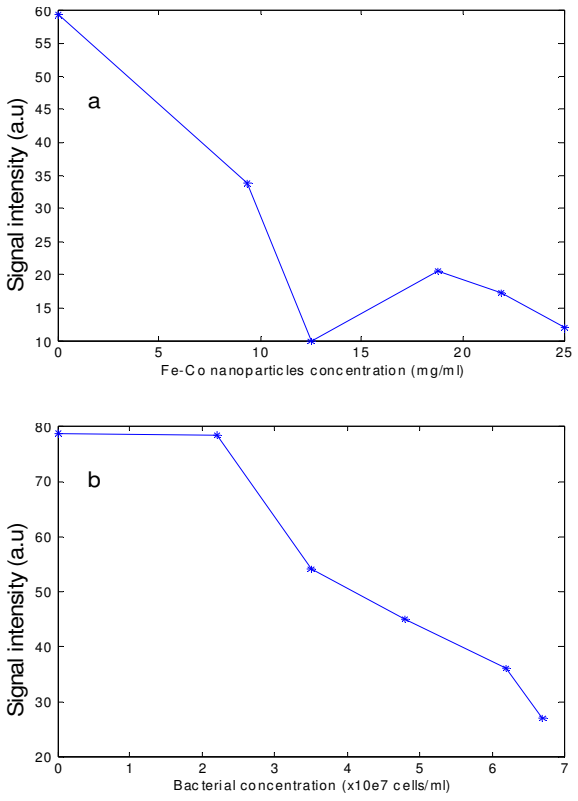

Fig. 2. Signal intensity as a function of the (a) Fe-Co nanoparticles concentration and (b) MTB concentrations.

2.

C. *T2-relaxation Curves*

The T_2 relaxation time for different concentrations of nanoparticles and MTB were calculated from signal ratio measurements as depicted in table 1. T_2-relaxation curves are plotted in Figure 3. Because of the severe signal loss, the T_2 relaxation value was not calculated for the Fe_3O_4 microparticles. However a rough estimate was calculated for the medium and the two less concentrated samples as depicted by Figure 3c.

IV. DISCUSSION

In the prospect of drug delivery applications, the problematic related to the MR-tracking depends on the concentration of the magnetic particles, their size as well as their magnetization. In the case of ferromagnetic microparticles, if the concentration is high, image artifact can cause misleading steering procedure causing drug delivery particles to miss a specific or target arteriole entry. In this particular case, an off-resonance sequence [9] would perform better for tracking purpose than T_1 or T_2 contrast. T_1 contrast can be effectively used after the agglomeration of microparticles diffuses through the arterioles-capillaries network. Nanoparticles and MTB cause moderate T_1 and T_2 change allowing them to be efficiently tracked at high concentrations but less at low concentrations.

The T_2 relaxation curves of Figure 2a help to find the echo time that gives the best contrast between tissues containing the magnetic particles and the surroundings. We can notice that the distance between the relaxation curves for different concentration of MTB becomes larger for higher echo time, which is not the case for the concentrations used for Fe-Co nanoparticles.

Estimate of magnetic particles concentration could be obtained by inverting the mathematical relation between the relaxation times and the relaxivity of the compound given by

$$\frac{1}{T_i} = \frac{1}{T_{i,0}} + \alpha_i c; \qquad i = 1,2 \tag{3}$$

where $T_{i,0}$ (s) is the relaxation rate of the medium, c (mg Fe/mL) is the concentration of the magnetic particles and α_i is the relaxivity expressed in $ms^{-1}(mg\ Fe/mL)^{-1}$ a property specific to the contrast agents [10].

These particles are investigated to mimic the behavior of polymeric microparticles loaded with magnetic nanoparticles and drug for cancer treatment. Magnetic properties of these microparticles can be very interesting for tracking their displacement in the blood vessels and their accumulation in organs. The magnetic signal allows us to know where the

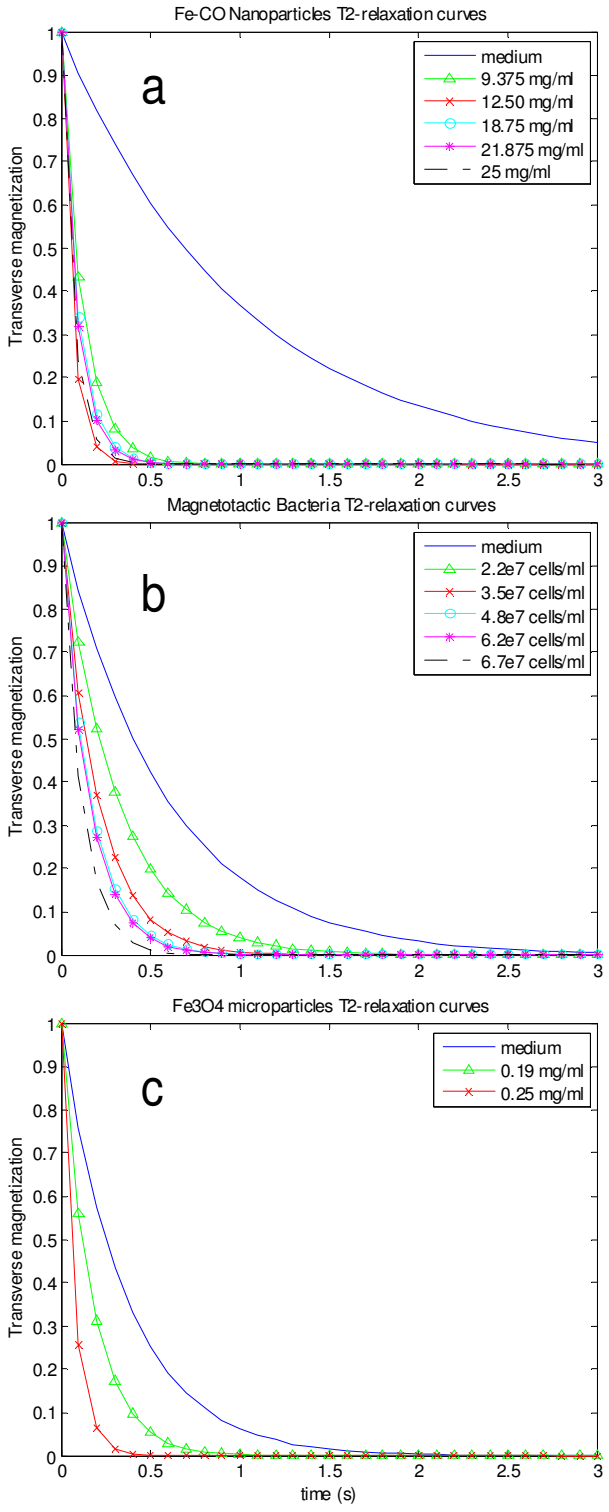

Fig. 3. T_2-relaxation curves for different (a) Fe-Co nanoparticles concentrations (b) MTB concentrations (c) Fe_3O_4 microparticles concentrations.

majority of drug is released in the body. For controlling the release of the drug, the polymeric matrix can be degradated by time [11] or by thermal effects [12]. In the case of polymeric microparticles loaded with high quantity of magnetic nanoparticles, it can be possible to control microparticles accumulation in a targeted organ by using strong magnetic gradients. For this application it is necessary to determine the quality of images generated by magnetic microparticles. Fe_3O_4 microparticles tested generate artefacts on MRI images. Despite that the magnetization of these microparticles is higher than one's obtained with polymeric microparticles loaded with iron oxide nanoparticles [13], image distortions have to be solved before *in vivo* trials. Furthermore, our team has already developed a tracking method based on the magnetic signature of a ferromagnetic core. The method has to be updated for a high concentration of magnetic microparticles suspensions.

Iron cobalt nanoparticles produce excellent negative contrast. This result is in good agreement with previous ones reported in the literature [14]. Iron cobalt nanoparticles surface can be modified by adding antibody ligands for cancer diagnostic. One major advantage for using these nanoparticles is that the injected dose can be less than iron oxide nanoparticles. Iron cobalt nanoparticles can be incorporated in polymeric micelles for drug delivery system [15].

MTB has the advantage to be self propelled and only need weak field in order to be oriented. However, the thrust of these microorganisms is estimated to be 4 pN [16], which mean that the blood flow is too high to be supported by the MTB. One solution to this problem is to use the MTB at the same time as the emboli-magnetic particles, such as the Fe_3O_4 microparticles used in this study. In this case, MTB will help to uniformly invade the tumor while the emboli-particles will stop the blood flow to the tumor.

V. Conclusion

These materials offer different magnetic properties, strategies for navigation and imaging parameters that can be combined in a single application where MRI could play a key role in a delivery procedure. Furthermore, T_1 and T_2 relaxivity values must be measured in order to relate the relaxation parameters to the concentration of the carrier.

Acknowledgment

We acknowledge Klaus Wojczykowski (Inorganic Chemistry III laboratory of Bielefeld University, Germany) for supplying Fe-Co nanoparticles and the Fonds Québécois de Recherche sur la Nature et les Technologies (FQRNT).

References

[1] E.P. Furlani, K.C. Ng, "Analytical model of magnetic nanoparticle transport and capture in the microvasculature," *Physical Review E,* vol. 73, n. 6, 2006.

[2] S. Martel et al., "Automatic navigation of an untethered device in the artery of a living animal using a conventional clinical magnetic resonance imaging system," *Applied Physics Letters*, vol. 90, no. 10, March, 2007.

[3] J.-B. Mathieu, G. Beaudoin, S. Martel, "Method of propulsion of a ferromagnetic core in the cardiovascular system through magnetic gradients generated by an MRI system" *IEEE Trans. Biomedical Engineering,* vol. 53, no. 2, pp. 292-299, Feb. 2006.

[4] R. P. Blakemore, "Magnetotactic Bacteria," *Science*, vol. 190, n. 4212, 1975.

[5] R. W. Kasinskas, N. S. Forbes, "Salmonella typhimurium specifically chemotax and proliferate in heterogeneous tumor tissue in vitro," Biotechnology and Bioengineering, vol. 94, n.4, pp. 710-721, 2006.

[6] A. Hutten and al., "Ferromagnetic FeCo nanoparticles for biotechnology," *Journal of Magnetism and Magnetic Materials*, vol. 293, n. 1, 2005.

[7] T. J. Williams, and al., "Evidence for autotrophy via the reverse tricarboxylic acid cycle in the marine magnetotactic coccus strain MC-1," *Applied and Environmental Microbiology*, vol. 72, n. 2, pp. 1322-1329, Feb. 2006.

[8] Bangs Laboratories, Inc. (www.bangslabs.com)

[9] C.H. Cunningham and al., "Positive contrast magnetic resonance imaging of cells labeled with magnetic nanoparticles," *Magnetic Resonance in Medicine*, vol. 53, n. 5, 2005.

[10] E. Toth, L. Helm, A. E. Merbach, "Relaxivity of MRI contrast agents," *Topics in Current Chemistry*, vol. 221(Contrast Agents I), pp. 61-101, 2002.

[11] X. Liu, M.D. Kaminski, H. Chen, M. Torno, L. Taylor, and A. J. Rosengart, "Synthesis and characterization of highly-magnetic biodegradable poly(d,l-lactide-co-glycolide) nanospheres," *Journal of Controlled Release*, vol. 119, n. 1, pp. 52-58, 2007.

[12] A. M. Ponce, Z. Vujaskovic, F. Yuan, D. Needham, and M. W. Dewhirst, "Hyperthermia mediated liposomal drug delivery," *International Journal of Hyperthermia*, vol. 22, n. 3, pp. 205-13, May, 2006.

[13] Y. Sun, B. Wang, H. Wang, and J. Jiang, "Controllable preparation of magnetic polymer microspheres with different morphologies by miniemulsion polymerization," *Journal of Colloid and Interface Science*, vol. 308, no. 2, pp. 332-336, 2007.

[14] W. S. Seo, J. H. Lee, X. Sun, Y. Suzuki, D. Mann, Z. Liu, M. Terashima, P. C. Yang, M. V. McConnell, D. G. Nishimura, and H. Dai, "FeCo/graphitic-shell nanocrystals as advanced magnetic resonance imaging and near-infrared agents," *Nature Materials*, vol. 5, n. 12, pp. 971-976, 2006.

[15] N. Nasongkla, E. Bey, J. Ren, H. Ai, C. Khemtong, J. S. Guthi, S.-F. Chin, A. D. Sherry, D. A. Boothman, and J. Gao, "Multifunctional polymeric micelles as cancer-targeted, MRI-ultrasensitive drug delivery systems," *Nano Letters*, vol. 6, n. 11, pp. 2427-2430, 2006.

[16] S. Martel, C. C. Tremblay, S. Ngakeng, G. Langlois, "Controlled manipulation and actuation of micro-objects with magnetotactic bacteria," *Applied Physics Letters*, vol. 89, n. 23, 2006.